Available online at www.sciencedirect.com
ScienceDirect
Ceramics International 38S (2012) S373–S377
CERAMICS INTERNATIONAL
www.elsevier.com/locate/ceramint

Effect of WO_3 doping on dielectric and ferroelectric properties of $0.94(Bi_{0.5}Na_{0.5})TiO_3$–$0.06BaTiO_3$ ceramics

Haiqin Sun, Xusheng Wang *, Xi Yao

Functional Materials Research Laboratory, Tongji University, Shanghai 200092, China

Available online 12 May 2011

Abstract

WO_3(0–6 mol%)-doped $0.94Bi_{0.5}Na_{0.5}TiO_3$–$0.06BaTiO_3$ lead-free ceramics were synthesized by conventional solid-state reaction. The effect of WO_3 addition on the structure and electrical properties were investigated. The result revealed that a small amount of WO_3 ($\leq$1 mol%) can diffuse into the lattice and does not significantly affect the phase structure, however, more addition will result in distortion and enlargement of the unit cells. The maximum permittivity temperature (T_m) is suppressed dramatically as the dopant increasing, while the depolarization temperature (T_d) fall to the minimum with 1 mol% WO_3 additive. The remanent polarization (P_r) was enhanced and coercive field (E_c) was reduced by doping with WO_3. The strain shows the largest value for 1 mol% doped sample, which is due to a field-induced antiferroelectric–ferroelectric phase transition.

Keywords: A. Powders: solid state reaction; C. Electrical properties; Strain; Field-induced

1. Introduction

Ferroelectric materials of the perovskite family (ABO_3-type) have received considerable attentions for the past several years owing to their promising potentials for various electronic devices such as multilayer capacitors (MLCCs), piezoelectric transducers, pyroelectric detectors/sensors, electrostrictive actuators, precision micropositioners, MEMS, etc. The most widely used ferroelectric materials are lead zirconate titanate based ceramics (PZT system). However, volatilization of toxic PbO during high temperature sintering not only causes environmental pollution but also generates unstability of composition and electrical properties of products. Therefore, lead-free ferroelectric materials have been attracting attention as new materials in place of PZT materials [1].

Bismuth sodium titanate ($Bi_{0.5}Na_{0.5}$)TiO_3 (BNT) is considered to be a promising candidate of lead-free materials. It is a perovskite ferroelectric relaxation material and shows strong ferroelectric properties at room temperature: relatively large remanent polarization (P_r = 38 μC/cm^2) and high Curie temperature (T_c = 320 °C). However, pure BNT ceramic is difficult to be polarized due to its large coercive field (E_c = 73 kV/cm) [2,3]. In order to solve this poling problem, varieties of BNT-based solid solutions have been studied recently, such as BNT–$PbTiO_3$ [4], BNT–$BaTiO_3$ [5] BNT–$SrTiO_3$ [6], BNT–$CaTiO_3$ [7], BNT–$Bi_{0.5}K_{0.5}TiO_3$ [8], BNT–$NaNbO_3$ [9] and BNT–$BiFeO_3$ [10]. Among them, the $(Na_{0.5}Bi_{0.5})_{1-x}Ba_xTiO_3$ (BNT–BT) system has attracted considerable attention on account of the existence of a rhombohedral–tetragonal morphotropic phase boundary (MPB) near x = 0.06. Compared with pure BNT, the $(Bi_{0.5}Na_{0.5})_{0.94}Ba_{0.06}TiO_3$ (abbreviated as BNBT6) compositions provide obviously decreased coercive field and substantially improved piezoelectric properties. Many further improvements on the electric properties of BNBT6 ceramics have been done by introducing small amount of oxide additives such as La_2O_3, Y_2O_3 [11,12]. And, different additives have different effects on the electrical properties, depending on the nature of the oxide additives and their substitution conditions.

The research of WO_3 doped BNBT6 ceramics has been rarely reported to date. Therefore, in present study, WO_3 doped BNBT6 lead-free piezoelectric ceramics were prepared and the effect of WO_3 addition on microstructure, dielectric, ferroelectric and piezoelectric properties was investigated.

* Corresponding author. Tel.: +86 21 65980544; fax: +86 21 65985179.
E-mail address: xs-wang@tongji.edu.cn (X. Wang).

0272-8842/$36.00
doi:10.1016/j.ceramint.2011.05.015

2. Experimental

The $(Bi_{0.5}Na_{0.5})_{0.94}Ba_{0.06}TiO_3 + x$ mol% WO_3 ($x = 0, 0.5, 1, 2, 4, 6$) ceramics were prepared by the conventional ceramic fabrication technique. The starting raw materials, Bi_2O_3 (99%, Alfa Aesar), Na_2CO_3 (Tianjin Chemical Reagent, 99.95%), $BaCO_3$ (99.8%, Alfa Aesar), TiO_2 (99.9%, Alfa Aesar) and WO_3 (99.8%, Alfa Aesar) were weighed and milled using an agate mortar with addition of alcohol. The mixed powders were calcined in an alumina crucible at 820 °C for 4 h in air. Then, they were remilled and granulated with polyvinyl alcohol (PVA) as a binder. The obtained powders were pressed into 10-mm-diam pellets at 100 MPa. The compacted discs were sintered at 1180 °C for 2 h in air.

The microstructures of the sintered samples were examined by scanning electron microscope (SEM, JSM EMP-800, JEOL, Japan). X-ray diffraction (XRD, Bruker D8 Advanced, Germany) with Cu Kα radiation was employed to examine the phase identification. The sintered pellets were polished and printed with Ag paste on both surfaces as electrodes. The temperature dependences of dielectric constant and loss were investigated using a high-precision LCR meter (HP 4284A, Hewlett Packard Co.) in the temperature range 25–400 °C. Polarization–electric field (P–E) and strain–electric field (S–E) loops were measured using a precision ferroelectric/piezoelectric analyzer (Premier II, Radiant Technologies Inc.) for pellets placed in a silicone oil bath setup at room-temperature.

3. Results and discussion

Fig. 1 shows the X-ray diffraction (XRD) patterns of sintered samples of WO_3 doped BNBT6 ceramics in the 2θ range of 20–80°. A single perovskite phase was observed for the samples with a small amount of WO_3 ($\leq$1 mol%), then a second phase appeared with further addition. Meanwhile, SEM micrographs exhibited the similar character as shown in Fig. 2. At lower doping concentration of WO_3 ($\leq$1 mol%), all of the samples had a rather similar morphology, consisting of fine and uniform particles less than 2 μm. But at higher doping concentration (>1 mol%), the grain size become larger and air holes were observed.

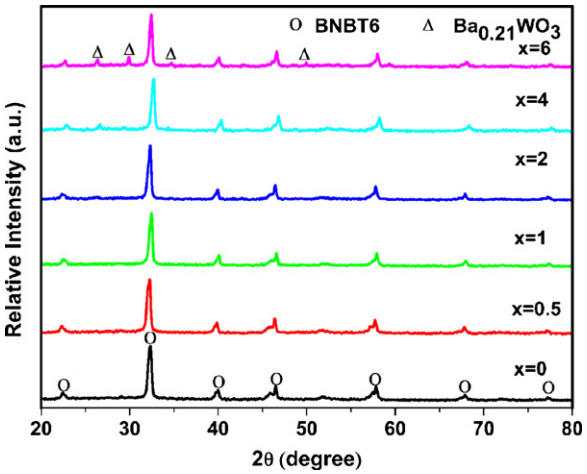

Fig. 1. X-ray diffraction patterns of BNBT6 with x mol% WO_3 ceramics.

According to Shannon's effective ionic radii, W^{6+} has a radius of 0.60 Å (C.N. = 6), which is close to that of Ti^{4+} (0.61 Å) [13]. Therefore, W^{6+} can enter into the B-site of the BNBT6 perovskite to substitute for Ti^{4+} because of radius matching and have less effect on grain size with increasing WO_3 amount when $x \leq 1$ mol%. On the other hand, an inverse effect of the W^{6+} substitution on crystal structure should also be taken into consideration. According to the theories of charge neutrality and crystal chemistry, the higher valence state of W^{6+} substitute the lower valence state of Ti^{4+} for the B-site of the ABO_3 structure will produce excess electron. To maintain an overall, titanium vacancies are created for compensation purposes. The generation of titanium vacancies result in a distortion and enlargement of the unit cells. From Fig. 2, one can suggest that the radius effect seems to be the main contributing factor at relatively low WO_3 amounts, while the titanium vacancy effect appears to be dominant at a higher WO_3 amounts. However, for excessive WO_3 doping (>2 mol%), above theories no longer functions well. So more and more titanium vacancies defects would been produced. As a consequence, the conductivity will be increasing eventually [14,15].

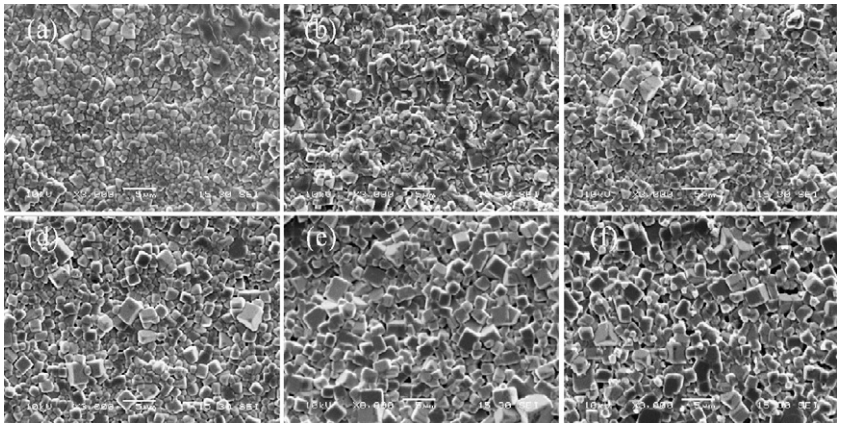

Fig. 2. SEM images of BNBT6 with x mol% WO_3 ceramics: (a) $x = 0$, (b) $x = 0.5$, (c) $x = 1$, (d) $x = 2$, (e) $x = 4$, (f) $x = 6$.

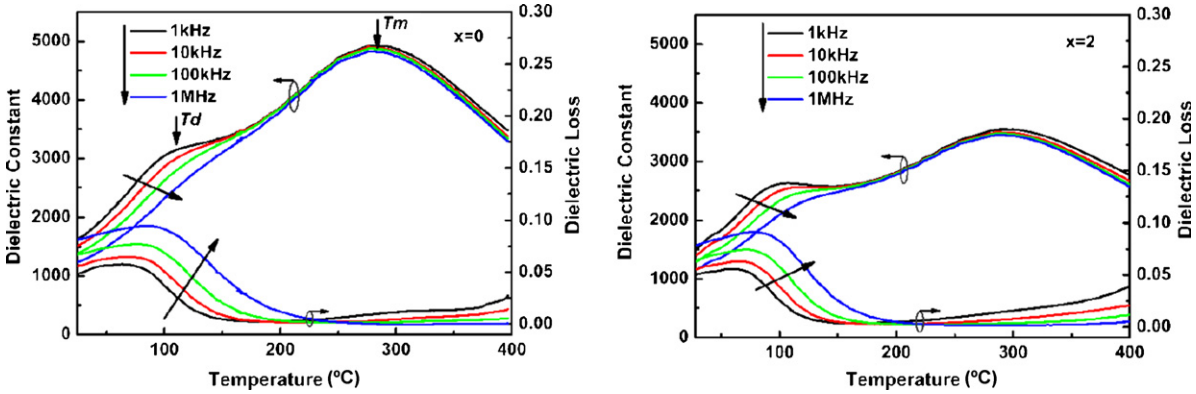

Fig. 3. Temperature dependence of dielectric constants and loss of BNBT6 with x mol% WO_3 ceramics with $x = 0$, $x = 2$.

Fig. 3 shows temperature dependence of dielectric constant and loss of pure BNBT6 and 2 mol% WO_3 doped sample only, because the curves for different samples look similar. All curves display two notable features: One is the shoulder at lower temperature, which is attributed to the phase transition from ferroelectric to antiferroelectric, whose onset point is called depolarization temperature (T_d). The other is a more clearly defined maximum peak at higher temperature, it is named as the maximum permittivity temperature (T_m), which is attributed to the transition from antiferroelectric to paraelectric, as indicated in Fig. 3 for $x = 0$. Both features are rather diffuse, the former exhibits a notable dependence on frequency, the latter is almost frequency independent for all compositions, which is consistent with a literature reported on BNT-based ceramics with a small amount of dopants or substitution [5,11].

Fig. 4 presents a direct comparison of the dielectric constant vs. temperature curves at a frequency of 10 kHz for WO_3 doped BNBT6 ceramics. The dielectric constant decreases and the dielectric–temperature curves become flatter with increasing WO_3. In particular, WO_3 doping level at 4 and 6 mol% caused the dielectric maximum to fall significantly. T_d gradually shifts to lower temperature up to a minimum value at 1 mol% WO_3 doped BNBT6, and then turn to higher temperature with further increasing amount of dopant. While, T_m depends far less on the doping level, it just has a small increase but not evident. The loss has not much change at room temperature with a certain additive content ($\leq$4 mol%), but at high temperature, it increases as the increment of WO_3-doping content. In particular, the loss for the 6 mol% WO_3 sample is obviously increased, which may be due to the large conduction.

The polarization vs. electric field hysteresis loops for all samples was measured, as shown in Fig. 5. The values of remanent polarization (P_r) and coercive field (E_c) derived from the P–E hysteresis loops can also be seen in Fig. 5. With WO_3 doping, the loops became slim. The P_r were enhanced ($x \leq 1$ mol%) and E_c were reduced ($x \leq 4$ mol%). For pure BNBT6 sample, the P–E hysteresis loop is saturated and exhibits a shape typical for ferroelectric. For 0.5 mol% and 1 mol% WO_3 doped samples, the loops appear ''pinched'', which is a characteristic feature of coexisting antiferroelectric domain and ferroelectric domain. This implies that antiferroelectric region exist in low level of WO_3 doping samples at room temperature due to the lower T_d. While, for 2 mol% and 4 mol% doped samples, the loops are saturated again, this maybe attribute to the increment of T_d that make the antiferroelectric region disappear at room temperature. For 6 mol% doped sample, the loop (not shown here) can not reach to saturation even by adding very high electric field, this may due to large conduction caused by heavy doped amount

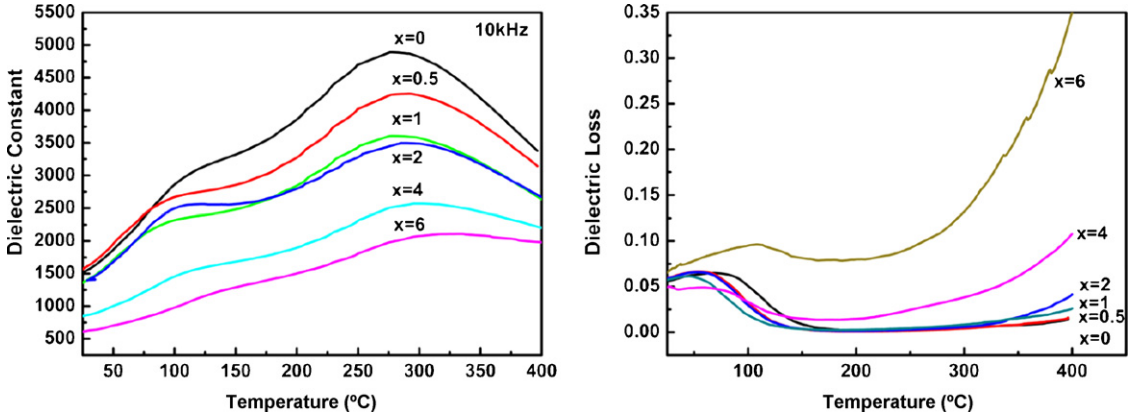

Fig. 4. The dielectric constant vs. temperature curves at a frequency of 10 kHz for BNBT6 with x mol% WO_3 ceramics.

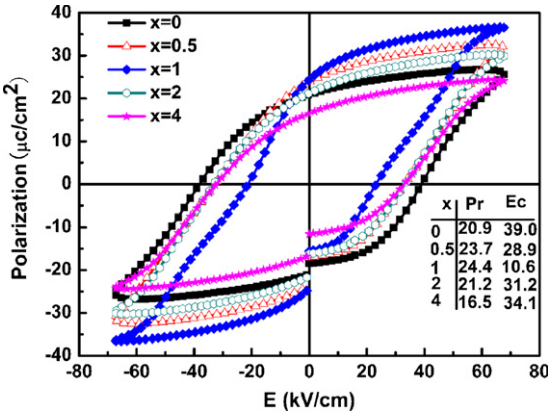

Fig. 5. The polarization vs. electric field hysteresis loops for BNBT6 with x mol% WO_3 ceramics.

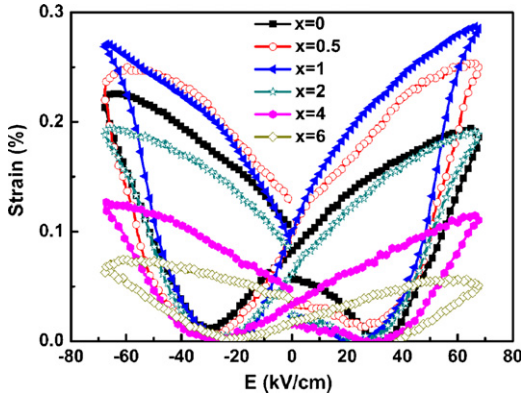

Fig. 6. The strain vs. electric field loops of BNBT6 with x mol% WO_3 ceramics.

of WO_3. This is consistent with phenomenon of dielectric constant vs. temperature curves in Fig. 4.

Fig. 6 displays the bipolar S–E curves of WO_3 doped BNBT6 samples. Noticeably, with the relatively low amount of added WO_3 ($\leq$1 mol%), the maximum strain is large than that of BNBT6 matrix. And the strain reaches to the largest value of about 0.27% when 1 mol% additive was doped. When WO_3 additive was beyond 1 mol%, the strain decrease as the doped level increase and became lower than that of the pure BNBT6. As mentioned above, the 0.5 mol% and 1 mol% doped sample have a pinched loop which imply the coexisting of antiferroelectric domain and ferroelectric domain. So, this large strain is caused by the field-induced antiferroelectric–ferroelectric phase transition and it is always higher than that which can be reached by the normal piezoelectric effect [16,17].

4. Conclusions

This study aims to investigate the doping effect of WO_3 on the microstructure and electrical properties of BNBT6 ceramics. BNBT6 ceramics doped with x mol% WO_3 (x = 0–6) were prepared by a conventional solid-state reaction route. A small amount of WO_3 ($\leq$1 mol%) does not significantly affect the phase structure and grain size. But the unit cells became distorted and enlarged with a heavy doping level. The maximum permittivity temperature T_m is suppressed dramatically and shift slightly as the doping level increasing, while the depolarization temperature T_d fall to the minimum for the 1 mol% WO_3 doped sample and then increased gradually with further doped amounts. The P_r were enhanced and E_c were reduced with a certain amount of WO_3. The 0.5 mol% and 1 mol% WO_3 doping induces antiferroelectric properties in the ceramic and lead to a relatively large maximum strain, which is due to a field-induced antiferroelectric–ferroelectric phase transition. This effect can be utilized in a wide temperature range.

Acknowledgements

This work was supported by the Natural Science Foundation of China (No. 50932007), Scientific and Technical Innovation Program of Shanghai (No. 08JC1419100) and Specialized Research Fund for the Doctoral Program of Higher Education (No. 20070247010).

References

[1] Y. Saito, H. Takao, T. Tani, T. Nonoyama, K. Takatori, T. Homma, T. Nagaya, M. Nakamura, Lead free piezoceramics, Nature 432 (2004) 84–87.
[2] G.A. Smolenskii, V.A. Isupov, A.I. Agranovskaya, N.N. Krainik, New ferroelectrics of complex composition, Soviet Physics Solid State 2 (1961) 2651–2654.
[3] C. Tu, I. Siny, V. Schmidt, Sequence of dielectric anomalies and high-temperature relaxation behavior in $Na_{1/2}Bi_{1/2}TiO_3$, Physical Review B 49 (1994) 11550–11559.
[4] S. Kuharuangrong, W. Schulze, Characterization of $Bi_{0.5}Na_{0.5}TiO_3$–$PbTiO_{3M}$ dielectric materials, Journal of the American Ceramic Society 79 (1996) 1273–1280.
[5] T. Takenaka, K. Muruyama, K. Sakata, $(Bi_{0.5}Na_{0.5})TiO_3$–$BaTiO_3$ system for lead free piezoelectric ceramics, Japanese Journal of Applied Physics 30 (1991) 2236–2239.
[6] K. Sakata, Y. Masuda, Ferroelectric and antiferroelectric properties of $(Na_{0.5}Bi_{0.5})TiO_3$–$SrTiO_3$ solid solution ceramics, Ferroelectrics 7 (1974) 347–349.
[7] T. Takenaka, K. Sakata, K. Toda, Acoustic wave characteristics of lead-free $(Bi_{0.5}Na_{0.5})_{0.99}Ca_{0.01}TiO_3$ piezoelectric ceramic, Japanese Journal of Applied Physics 28 (1989) 59–62.
[8] A. Sasaki, T. Chiba, Y. Mamiya, E. Otsuki, Dielectric and piezoelectric properties of $(Bi_{0.5}Na_{0.5})TiO_3$–$(Bi_{0.5}K_{0.5})TiO_3$ systems, Japanese Journal of Applied Physics 38 (1999) 5564–5567.
[9] T. Takenaka, T. Okuda, K. Takegahara, Lead-free piezoelectric ceramics based on $(Bi_{1/2}Na_{1/2})TiO_3$–$NaNbO_3$, Ferroelectrics 196 (1997) 175–178.
[10] H. Nagata, N. Koizumi, T. Takenaka, Lead-free piezoelectric ceramics of $(Bi_{0.5}Na_{0.5})TiO_3$–$BiFeO_3$ system, Key Engineering Materials 169 (1999) 37–40.
[11] P. Fu, Z. Xu, R. Chu, W. Li, G. Zang, J. Hao, Piezoelectric, ferroelectric and dielectric properties of La_2O_3-doped $(Bi_{0.5}Na_{0.5})_{0.94}Ba_{0.06}TiO_3$ lead-free ceramics, Materials & Design 31 (2010) 796–801.
[12] C Zhou, X. Liu, W. Li, C. Yuan, Dielectric and piezoelectric properties of Y_2O_3 doped $(Bi_{0.5}Na_{0.5})_{0.94}Ba_{0.06}TiO_3$ lead-free piezoelectric ceramics, Materials Research Bulletin 44 (2009) 724–727.
[13] R.D. Shannon, Revised effective ionic radii and systematic studies of interatomic distances in halides and chalcogenides, Acta Crystallogra-

phica Section A: Crystal Physics, Diffraction, Theoretical and General Crystallography 32 (1976) 751–767.

[14] Q. Xu, M. Chen, H.X. Liu, B.H. Kim, B.K. Ahn, Effect of CoO additive on structure and electrical properties of $(Na_{0.5}Bi_{0.5})_{0.93}Ba_{0.07}TiO_3$ ceramics prepared by the citrate method, Acta Materialia 56 (2008) 642–650.

[15] S. Shannigrahi, K. Yao, Effects of WO_3 dopant on the structure and electrical properties of $Pb_{0.97}La_{0.03}(Zr_{0.52}Ti_{0.48})O_3$ thin films, Applied Physics Letters 86 (2005) 092901.

[16] S. Zhang, A. Kounga, E. Aulbach, T. Granzow, W. Jo, H.J Kleebe, R. del, Lead-free piezoceramics with giant strain in the system $Bi_{0.5}Na_{0.5}TiO_3$–$BaTiO_3$–$K_{0.5}Na_{0.5}NbO_3$. I. Structure and room temperature properties, Journal of Applied Physics 103 (2008) 034107.

[17] S. Zhang, A. Kounga, E. Aulbach, W. Jo, T. Granzow, H.J Ehrenberg, R. del, Lead-free piezoceramics with giant strain in the system $Bi_{0.5}Na_{0.5}$-TiO_3–$BaTiO_3$–$K_{0.5}Na_{0.5}NbO_3$. II. Temperature dependent properties, Journal of Applied Physics 103 (2008) 034108.